Influence of Shot Peening Coverage on Residual stresses Induced in Aluminum Alloy 7050-T745

H. Bae[1], H. Diep[2] and M. Ramulu[1]

1Department of Mechanical Engineering, University of Washington, Seattle, USA
2The Boeing Company, Seattle, USA

ABSTRACT
Experimental investigation was conducted to study the residual stresses in aluminum alloy 7050-T745. A vacuum-blasting system from Vacublast was employed for this study. A 6 mm diameter nozzle and cast steel shots (S230) were used for the system. Type A Almen strips were used for Almen intensity measurements. Aluminum alloy 7050-T7451 blocks (100 mm X 100 mm) were used for shot peening coverage. Micro-hardness measurements were made and hole drilling techniques were used to measure the residual stresses on Al 7050-T745 specimens peened at four levels of coverage. This paper presents the results of experimental and anlytically estimated compressive residual stresses, which includes intensity and coverage effects.

Introduction

Residual stress and surface hardening induced by shot peening increase the fatigue life and the resistance to stress corrosion cracking within metallic components [1-12]. Surface hardening and compressive residual stress measurements can be a means to verify the shot peening effects. Even though shot peening has been used for more than 50 years, a review of published papers indicates a lack of studies for estimation of shot peening effects due to the complexity of the shot peening process in which target materials respond to the multiple impacts of shots. There exist a few handfuls of modeling fomulations to predict the residual stress [13-16]. However, most of the studies didn't include shot peening process effects on their compressive residual stress predictions. It was also reported that intensity and coverage have the greatest effect on the compressive residual stress and micro-hardness [7-11]. However, in manual peening processes, underpeening or overpeening areas can cause variable residual stress which results in fatigue life degradation of soft aerospace materials such as Al 7050-T7451.

The purpose of this paper is to present the experimental results of residual stress measurements by the Hole Drilling method for varying coverage and proposes an analytical compressive residual stress estimation method by including intensity and coverage effects. It relates the surface hardening effect and the yield strength to the residual stress. The estimation results are compared with residual stress measuments by the Hole Drilling method.

Experimental method

A vaccum-blasting system from Vacublast was employed for this study. A 6 mm diameter nozzle and cast steel shots (S230) were used for the system. Type A Almen strips were used for Almen intensity measurements. An image analysis system was introduced for coverage measurements [10-12]. Aluminum alloy 7050-T7451 blocks (100 mm X 100 mm) were used for shot peening coverage. 14 block specimens were peened at 14 different conditions and these conditions were combinations of three variables: SOD, air pressure, and Angle of impingement [10-12]. The material of the test block was Al 7050-T7451. Table 1 lists the typical chemical composition of Al 7050-T745 and Table 2 shows mechanical properties of Al 7050-T745 used in this study. Change of surface micro-hardness resulting from shot peening was evaluated by using a LECO AMH 43 Micro-hardness Testing System. Subsurface micro-hardness measurements were taken every 15 μm to a depth of 240 μm using 100 g load and 10 sec dwell time. The shot peening condition was cast steel shot S230, 172 kPa air pressure, 304 mm SOD, 90° impingement angle, 40.1 g/sec shot flow rate and 0.24 mm A (0.01 A) intensity with four coverages, 28.4%, 52.5%, 78%, and 100%. Carbide mill #38 FG Inverted cone and Strain gage type CEA-13-062UL-120 was used in Hole drilling experiments.

Table 1 Chemical Composition of Al 7050-T745 (wt. %) [17]

Mg	Cu	Zn	Zr	Mn	Fe	Si	Ti	Cr	Other	Al
1.9 to 2.6	2 to 2.6	5.7 to 6.7	0.08 to 0.15	0.1 max	0.15 max	0.12 max	0.06 max	0.04 max	0.15 max	Bal

Table 2 Mechanical properties of Al 7050-T745

Property	ASM[17]
Yield Strength (MPa)	469
Ultimate Tensile Strength (MPa)	524
Elongation (%)	11
Young's Modulus, E, (GPa)	71.7
Poisson's ratio	0.33
Fracture Toughness, K_{IC}, ($MPam^{1/2}$)	28
Density (Kg/m^3)	2830

Results and Discussion

Coverage and Intensity

Coverage analysis was evaluated by using optical micrographs and Image J program. Typical coverage micrographs of shot peened Al 7050 flat block are shown in Figure 1. The resulting coverages were 28.4%, 52.5%, 78%, and 100%, respectively.

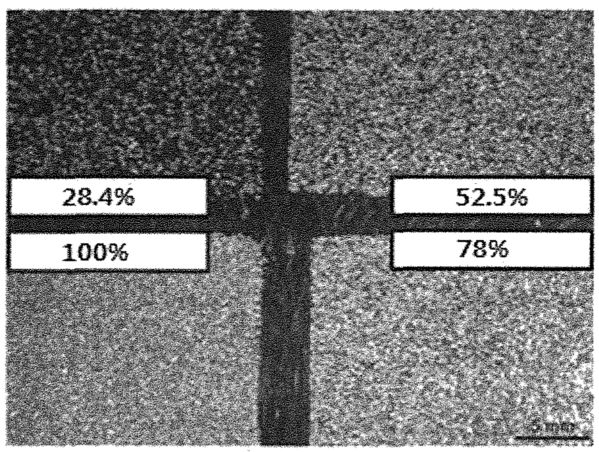

Figure 1 Typical shot peened Al 7050 flat block surfaces.

Higher intensities reduced the time to reach 100% coverage shown in Figure 2. In order to analyze the intensity effects on coverage, two samples were chosen among 14 samples. The pressures of two samples were only varied while the other conditions were held constant at the same conditions. The conditions were SOD (305 mm), impingement angle (60°), and two different pressures (103 kPa and 172 kPa). Two different pressures yields two different intensities, 0.14 mmA and 0.22 mmA. Figure 2 also shows the intensity effects on the coverage. It is clear that a higher intensity has less coverage time than a lower intensity because of higher velocity of shots.

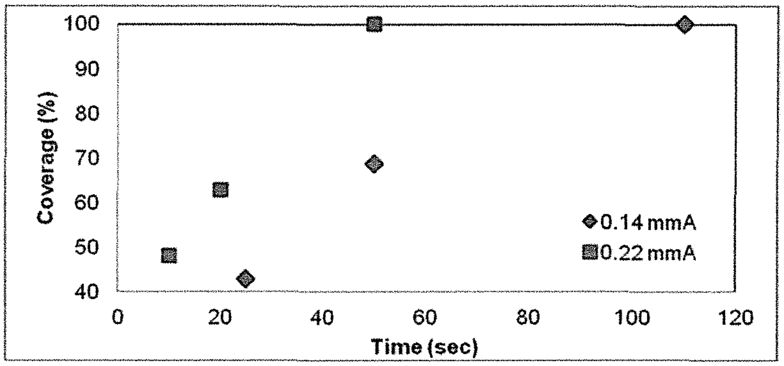

Figure 2 Intensity effect on coverage.

Microhardness

Fig. 3 shows the normalized subsurface micro-hardness data with various coverage conditions from 28.4% to 100%. Each data point is an average of three micro-hardness measurements. Note that the increase in hardness extends to a depth of 250 μm. The increase in surface hardness was about 10%. It is also observed that values of subsurface micro-hardness vary depending on degree of % coverage. It is clear that changes up to 100% coverage have a pronounced effect on the micro-hardness and very little effect at coverage greater than 28.4%.

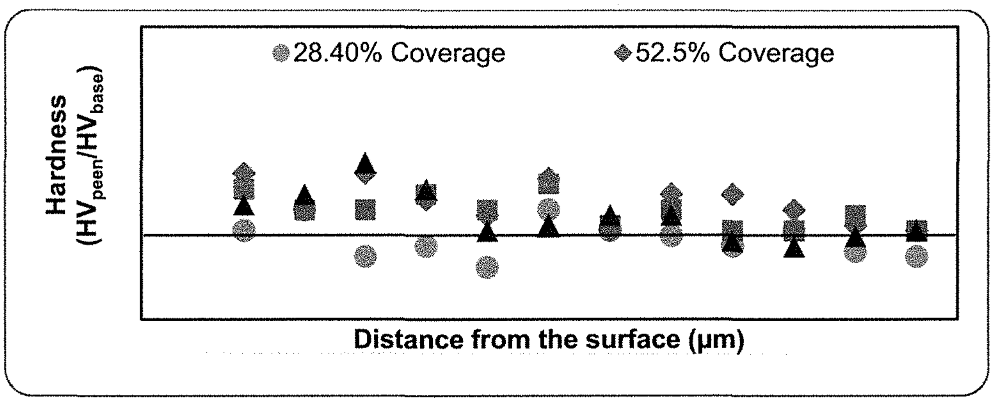

Figure 3 Normalized Hardness vs. distance from the edge surface (HV_{base} 100 g = 160).

Residual stresses

Stresses measured from the hole drilling method are shown in Figure 4. The 28.4% coverage shows the lowest magnitude of the compressive residual stress. An increase in the degree of % coverage causes an increase in the magnitude of the compressive residual stress. It is shown that magnitudes of compressive residual stresses from 52.5% to 100% are similar. However, an increase in the degree of % coverage induces increase in the width of compressive residual stress. It is shown that 100% coverage subsurface has the highest magnitude of maxiumum compressive residual stress and the widest width of the compressive residual stress profile.

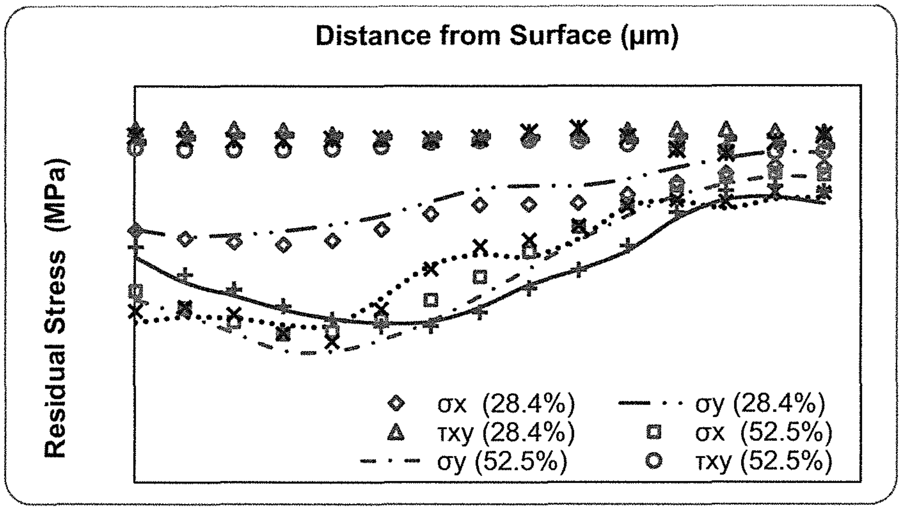

Figure 4 Stresses measured from Hole drilling method.

Semi-Analytical Modeling and Estimation

The compressive residual stress is directly related to the plastic strain induced in the shot peened layer. Furthermore, the cold work or work hardened layer is a measure of the irreversible plastic strain. Thus, estimation of the compressive residual stress of the shot peened layer can be made from the micro-hardness. The literature review shows that the plasticity effect becomes significant when the existing compressive residual stresses overcome 80% of the corresponding local yield strength of the peened material. Based on the proportionality between hardness and yield strength, the residual stress σ_R has been successfully determined using the yield strength of the bulk material σ_y and the relative variation of the micro-hardness according to the following relationship [18]:

$$\sigma_R = k \times \sigma_Y \left(1 + \frac{\Delta H_V}{Hv_{base}}\right) \quad (1)$$

where, σ_Y : Yield strength (470 MPa)

$0.6 < k < 0.8$

$\frac{\Delta H_V}{Hv_{base}}$: The relative variation of the micro-hardness

However, this calculation only gives the magnitude of the residual stress. Using a Gaussian type curve fitting model, the residual stress curve can be created. The Gaussian type curve fitting model is shown as:

$$\sigma_R = A \times exp\left[\frac{-2(x-\bar{x})^2}{W^2}\right] + B \quad (2)$$

where, σ_R: residual stress (MPa)

x: depth below the surface (mm)

A+B : maximum residual stress (MPa)

B: Preset residual stress (MPa)

W: the width of the residual stress curve (mm)

$\bar{x}$: depth of maximum residual stress (mm)

The result from Eq. 1 can be treated as maximum residual stress. Combining Eqs. 1 and 2 and incorporating a coverage and intensity effects as proportional constants reduces to:

$$\sigma_R = k_I \times k_C \times \sigma_Y \left(1 + \frac{\Delta H_V}{Hv_{base}}\right) \times exp\left[\frac{-2(x-\bar{x})^2}{W^2}\right] + B \quad (3)$$

where, k_I: Intensity coefficient and k_C: Coverage coefficient

Estimation of the compressive residual stress induced by shot peening treatment for a given coverage and intensity can be made by using Eq. 3. The *k* coefficients are depending on the intensity and coverage. So, it is necessary to determine the coefficient k_I and k_C. In order to determine the intensity coefficient k_I, previous experimental data of the authors were utilized, where the micro-hardness and the compressive residual stresses at the different intensities from 0.1 mm A (0.004 A) to 0.4 mm A (0.016 A) for aluminum alloy 7075-T7351 were measured [19, 20]. Using the micro-hardness data, the compressive residual stresses were estimated. The width of the compressive residual stress (W) and the depth of maximum residual stress were chosen from the micro hardness data. The preset residual stress (B) was chosen as 50 MPa from the measured residual stress of as-machined specimens. The range of estimated k_I coefficients was also met with the coefficient range ($0.6<k<0.8$) from the literature [8, 18]. The resulting k_I coefficents show the linear relation as in Equation 4 and coverage coefficient k_C as in Equation 5:

$$k_I = 1.38 \times I(mmA) + 0.35 \qquad (4).$$

$$k_C = 0.0051 \times C(\%) + 0.4306 \qquad (5)$$

Based on the estimation of the k_I coefficients, 0.24 mm A (0.01 A), the intensity is corresponding to 0.68 k_I coefficient for this study. 28.4%, 52.5%, 78%, and 100% coverages are also corresponding to 0.57, 0.7, 0.83, and 0.94 k_C coeffecients. the estimated compressive residual stress curves were generated by all the obtained results. The width of the compressive residual stress (W) and the depth of maximum residual stress were chosen from the measured micro-hardness data: 100 µm the depth of maximum hardness ($\bar{x}$), 250 µm the width of the micro-hardness curve (W), and 0 MPa preset residual stress (B).
The result of the experimental and semi-empirical estimated compressive residual stress are shown in Figure 5. It is observed that the coverage and intensity changes induce the change of magnitude of the compressive residual stress.

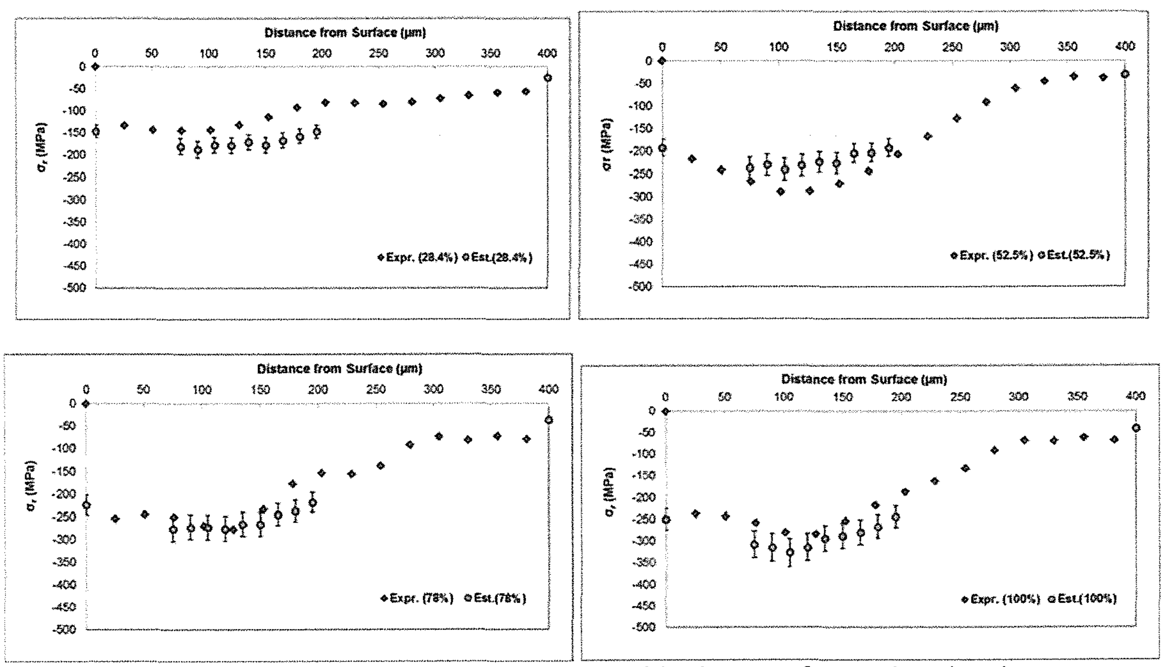

Figure 5 Estimation of the compressive residual stress from micro-hardness.

Summary
The analytical estimation of the compressive residual stress was developed in this study. The compressive residual stress was estimated from the experimentally measured subsurface micro-hardness data. Intensity and coverage effects were successfully included by this estimation. It was observed that higher intensity and higher coverage yield a higher degree of compressive residual stress and micro-hardness.

References

[1] A. Niku-Lari: *Shot-Peening*, First Int'l. Conf. On Shot Peening (1981), p. 395-403.

[2] J. Champaigne: *Shot Peening Overview*, Electronics Inc. (2001).

[3] D. Kirk: *Shot Peening*, Aircraft Engineering And Aerospace Technology, Vol71 (1999), p. 349-361.

[4] D. Kirk: *Effects of Varying Shot Peening Impact Angle*, The Shot Peener (2005), p. 28-31.

[5] R. Mcfarland: *Role Of Shot Peening Processes In Helicopter Component Qualification And Repair*, The 9th Joint FAA/DOD/NASA Conference On Aging Aircraft (2006).

[6] A. Biggs: *Analysis Of Factors Affecting Almen Strip Arc Height After Shot Peening*, M. S. Thesis University Of Washington (1999).

[7] T. Ludian and L. Wagner: *Coverage Effects In Shot Peening Of 2024-T4*, 9th Int'l. Conf. on Shot Peening (2007), p. 296-301.

[8] L. Wagner: *Mechanical Surface Treatments On Titanium, Aluminum And Magnesium Alloy*, Material Science And Engineering, Vol. A263 (1999), p. 210-216.

[9] T. Dorr and L. Wagner: *Effect Of Shot Peening On Residual Life Of Fatigue Pre-Damaged 2024 Al*, Sixth Int'l. Conf. On Shot Peening (1996).

[10] H.Diep, H. Bae And M. Ramulu: *Characterization Of Manual Shot Peening Process: Preliminary Results*, 10th Int'l. Conf. On Shot Peening (2008).

[11] H. Bae And M. Ramulu: *Effects Of Manual Shot Peening Conditions On High Cycle Fatigue In Aerospace Material*, Proceedings of the SEM Annual Conference (2009).

[12] Davis, J., H. Bae, and M. Ramulu: *Theoretical and Experimental Study of Coverage in Manual Shot Peening*, 11th Int'l. Conf. On Shot Peening (2011).

[13] S.T.S. Al-Hassani: *Mechanical aspects of residual stress development in shot peening*, First Int'l. Conf. on Shot Peening (1981), p. 583-602.

[14] R. Fathallah: *Modeling of shot peening residual stresses and plastic deformation induced in metallic parts*, Sixth Int'l. Conf. on Shot Peening (1996).

[15] H. Guechichi, L. Castex, J. Frelat, G. Inglebert: *Predicting residual stresses due to shot peening*, Impact Surface Treatment, edited by S. A. Meguid, Elsevier, Applied Science Publishers LTD (1986).

[16] J.K. Li, Y. Mei, W. Duo: *Mechanical approach to the residual stress field induced by shot peening*, Material Science and Engineering, A147 (1991), p. 167-173.

[17] Metals Handbook, Vol.2 - Properties and Selection: Nonferrous Alloys and Special-Purpose Materials, ASM International 10th Ed.

[18] P. Nobre, M. Kornmeier, A.M. Dias and B. Scholtes: *Comparative Analysis Of Shot-Peening Residual Stresses Using Hole-Drilling And X-Ray Diffraction Methods*, Materials Science Forum. Vol. 347-349 (2000), p. 138-143.

[19] T. Honda, M. Ramulu, and A.S. Kobayashi: *Shot Peening And Fatigue Crack Growth In 7075-T7351 Aluminum*, Key Engineering Materials 297 (2005), p. 72-77.

[20] T. Honda, M. Ramulu, and A.S. Kobayashi: Fatigue Of Shot Peened 7075-T7351 Senb Specimen–A 3D Analysis, Fatigue & Fracture of Engineering Materials & Structures 29.6 (2006), p. 416-424.